jESE

Original scientific paper

Ellipsometric measurement of thickness of tin oxides grown by voltammetry in phosphate solution of pH 8.7

Tiago Brandão Costa*,✉, Tania Maria Cavalcanti Nogueira*,**, Ladário da Silva*,***

*Programa de Pós-Graduação em Engenharia Metalúrgica (PPGEM), Escola de Engenharia Industrial Metalúrgica de Volta Redonda (EEIMVR), Universidade Federal Fluminense (UFF), 27255-125 Volta Redonda, RJ, Brazil
**Departamento de Metalurgia, EEIMVR, UFF, 27255-125 Volta Redonda, RJ, Brazil
***Departamento de Física, Instituto de Ciências Exatas (ICEx), UFF, 27213-145 Volta Redonda, RJ, Brazil

✉Corresponding author: tiagobrandao@id.uff.br, Phone: +55-2421073731

Abstract

The voltammetry induced growth of tin oxides on tin in the buffer solution of 0.18 mol L^{-1} Na$_2$H$_2$PO$_4$ and 0.18 mol L^{-1} KH$_2$PO$_4$ (pH 8.7) has been studied. Ex-situ ellipsometric measurements were made in an order to determine thicknesses of the grown oxides. From these results the film volume per charge unit, V$_f$, was calculated for different charge densities of the film. This parameter was used to calculate the variable ionic resistivity of the film, ρ$_f$, considered by the Ohmic model for the case of voltammetric growth of oxides on metals having a previously existing continuous film. Tin oxide films grown at 2 mV s^{-1} showed to be less dense for values of charge density below 50 C m^{-2}, having V$_f$ near 5.7x10^{-10} m^3 C^{-1}. For higher values of charge density, tin oxide films become denser, having V$_f$ near 0.5x10^{-10} m^3 C^{-1}. The calculated values of the variable ionic resistivity of the film during voltammetric growth showed that ρ$_f$ passes through a minimum (justifying the maximum in current densities). This behavior was also found by other authors in the cases of Zn, Nb, Ni and galvanized steel sheets.

Keywords

Ellipsometry, Tin oxide, Ohmic model, Voltammetry, Variable ionic resistivity

Introduction

Active metals cannot be obtained without an initial thin film covering the surface, as have already been observed in the cases of Cd, Fe, Ni, Pb, Sn, Zn, valve metals, *etc*. For this reason, the studies of oxide growth on these metals are found very important. The growth of passivating films on metals

under voltammetric conditions gives rise to peaks or polarographic waves in current/potential plots. This phenomenon is related to the active/passive transition, or growth of a continuous film on the metal surface.

Some electrochemical processes, such as electrodeposition of metallic ions [1–3] or growth of oxide on metals [4–8], can be considered as processes presenting ohmic behaviour. The Ohmic model developed by D'Alkaine [4] describes the relation between the current density and the film overpotential during the growth of passivating film under voltammetric conditions. This model considers that the relation between the electrode potential E and overpotential at the metal/film/solution interface is given by:

$$E = \eta_{m/f} + \eta_f + E_F \tag{1}$$

In Eq. (1) $\eta_{m/f}$ is the overpotential at the metal/film interface, η_f is the overpotential across the film and E_F is the Flade potential. The overpotential at the film/solution interface is considered constant, *i.e.* independent of the current density, j.

The relation between current density (j) and overpotential at the metal/film interface ($\eta_{m/f}$) is given by the general expression:

$$j = j_{m/f}^0 \left[\exp\left(\alpha_a n f \eta_{m/f}\right) - \exp\left\{-\left(\alpha_c n f \eta_{m/f}\right)\right\} \right] \tag{2}$$

In Eq. (2), $j_{m/f}^0$ is the exchange current density at zero $\eta_{m/f}$, f is F/RT, α_a and α_c are anodic and cathodic transfer coefficients, while n is charge of the metal ion in the film.

If V_f and q_f are respectively the volume per charge unit and the charge density related to the growing film, then the film thickness, ℓ, is given by:

$$\ell = V_f q_f \tag{3}$$

The q_f value can be calculated as:

$$q_f = q_{volt} + q_0 = \frac{1}{v} \int_{E_i}^{E} j_a dE + q_0 \tag{4}$$

In Eq. (4) q_0 is the charge density related to the amount of film initially present at the beginning of the voltammetric growth and q_{volt} is the charge density related to the amount of film which has grown on the metal surface during the voltammetric experiment. E_i is the initial potential, E is the potential attained and j_a is anodic component of the current density, taking into account Eq. (2).

For peak or plateau, transient conditions during voltammetric growth of a film on a metal surface, the following equation should be valid for any model:

$$\eta_{f,p} = \frac{v}{j_p} q_{f,p} \tag{5}$$

In Eq. (5) $\eta_{f,p}$ is the overpotential across the film at the voltammetric peak, v is the sweep rate, j_p is the current density at the peak and $q_{f,p}$ is the peak or plateau charge density.

In the case of the Ohmic model, the relation between j and η_f, even at high fields, is given as:

$$\eta_f = V_f \rho_f q_f j \tag{6}$$

In Eq. (6), ρ_f is the average ionic specific resistivity of the film.

The Ohmic model takes into consideration that at the beginning of the scanning, the current density increases as a consequence of reduction of ionic resistivity of the film due to injection of defects in the film. Beyond the peak potential, it is possible to observe reduction of the current

density, what is explained by ageing of the oxide film. This phenomenon turns the film more resistive to the passage of the current due to recombination of defects and to structural rearrangement [4]. This model, however, contains an intrinsic difficulty related to impossibility to determine ρ_f and V_f separately, using only electrochemical measurements. Despite this fact, many authors [4−8] applied the Ohmic model, considering the volume per charge unit (V_f) as the constant equal to:

$$V_f = \frac{M}{nF\delta}$$ (7)

In Eq. (7) M is the molar mass of the film, δ is density of the film, n is the number of electrons and F is the Faraday's constant.

The real values of V_f during the voltammetric growth could only be determined by independent measurements of the film thickness. The aim of the present work is to study the voltammetric growth of tin oxides in a solution of phosphate (pH 8.7) applying the Ohmic model. This solution was chosen in view of stability of the passive film on tin at this pH, avoiding thus loss by chemical dissolution [9]. At the same time, there are some early studies concerning the passivating species under voltammetric growing conditions in the pH range 8–9 [10–14]. The thickness of the oxides grown by voltammetry will be determined by ex-situ ellipsometric measurements in an order to verify the intrinsic difficulty explained above. The ex-situ condition was first examined as a preliminary study in order to verify stability of the film in the atmosphere.

Experimental

Electrochemical measurements

The working electrode was made of a tin disc (99.999 % of purity) with the circular area of 50 μm^2. Before the experiments, the electrode surface was polished with 600-emery paper.

The electrochemical experiments were performed using the EG&G Princeton Applied Research Model 273A potentiostat. Reagents PA and purified water (Millipore Q system) were used. The electrolyte solution was 0.18 mol L^{-1} Na$_2$H$_2$PO$_4$ + 0.18 mol L^{-1} KH$_2$PO$_4$, pH 8.7. The experiments were carried out in a conventional three-compartment electrolysis cell, using a platinum wire as the counter and Hg/Hg$_2$Cl$_2$/KCl (1 M) as the reference electrode, respectively.

All current and charge densities are given in terms of the geometric surface area of the analyzed samples.

Anodic voltammetries were carried out at sweep rates of 2, 5, 10, 20, 70, 100, 200, 300 and 400 mV s^{-1}, always using the same sample. For this purpose, before each voltammetry experiment, the previously grown oxide film was reduced at constant cathodic potential equal to -1.2 V during 600 s. After this treatment, the obtained voltammograms were reproducible, indicating that surface roughness of samples was also reproducible.

Ellipsometric measurements

Ellipsometry [15] is a powerful and non-destructive technique, which allows one to access optical and dielectric properties of various materials in different forms (solids, liquids, and gases), as well as thicknesses of thin films [16−17]. It can also be used to monitor and analyze both in-situ [18−19] and ex-situ [20] experiments. Ellipsometry considers the change in the polarization state of incident light upon reflection from the studied material. Initially it accesses the ellipsometric parameters Ψ and Δ. These parameters are connected by the fundamental equation of ellipsometry [16]:

$$\frac{R_p}{R_s} = \tan(\psi)e^{i\Delta} = f(n_j, k_j, d_j) \tag{8}$$

In Eq. (8), R_p and R_s stand for the complex Fresnel reflection coefficients for p and s polarized light beams, respectively. Ψ is the amplitude ratio for the reflected and polarized components (p and s), while Δ represents the phase difference between reflected p and s polarizations, created by reflection from the material. n_j, k_j, d_j are, respectively, the refractive index, the extinction coefficient and thickness of the jth layer of the material. The ex-situ ellipsometric measurements were made using a SEMILAB spectroscopic ellipsometer, model SOPRA GES 5E, equipped with a Xe lamp, over the spectrum range of 195 – 1,000 nm. The investigation of the thickness of oxide films grown on the substrate of tin has been performed in air and at ambient temperature using the incident angle of 75°. As an indirect technique, it is necessary to model the material structure with its film layers in an order to obtain each layer film thickness. The thicknesses of the oxide films were obtained by analyzing the measured ellipsometric spectra through the Drude and Gauss model [16].

Results and discussion

As was explained before, in an order to obtain reproducibility, the voltammetric experiments were always carried out using the same sample. Before each voltammetry measurement, the oxide grown in the previous experiment was reduced at the constant cathodic potential during 600 s. This cathodic treatment was sufficient to reproduce the initial roughness of the surface, which was verified by reproducible voltammograms obtained at the same sweep rate and shown in Fig. 1.
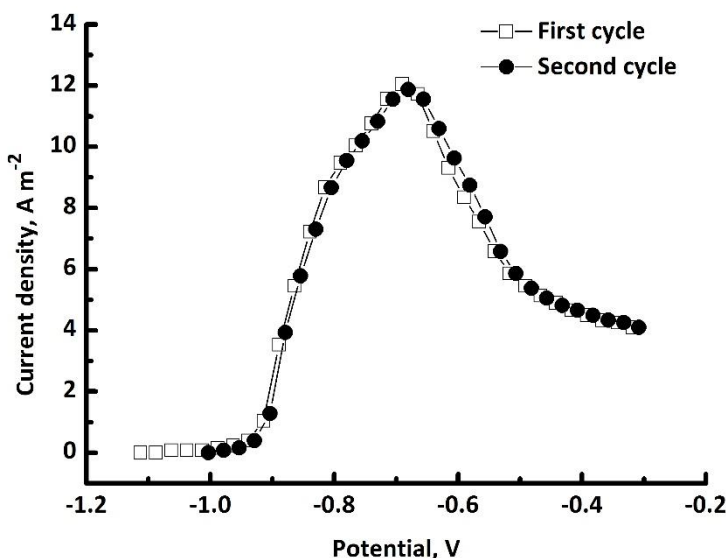

Fig. 1. *First and second cycle at 50 mV s^{-1} in the phosphate solution pH 8.7*

The anodic voltammograms for tin oxide growth at different sweep rates are shown in Fig. 2. From these results, the overpotential values in the film at the peak condition ($\eta_{f,p}$) were calculated using the Eq. (5). The value of q_0 in Eq. (4) was first considered equal to 0.0 C m^{-2}. The curve j vs. potential at the metal/film interface ($E_{m/f}$), also shown in this Figure, is obtained after correction of the ohmic drop through the film at the peak potential ($E_p - \eta_{f,p}$).
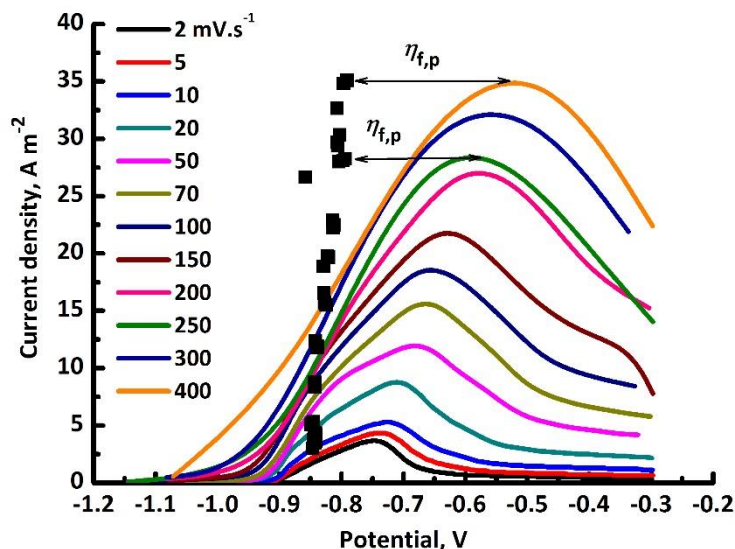
Fig. 2. *Voltammetric growths of tin oxide film, together with the plot of the calculated* j *vs. (*$E_p − \eta_{f,p}$*) relation at the metal/film interface, considering* q$_0$ *= 0.0 C m^{-2}.*

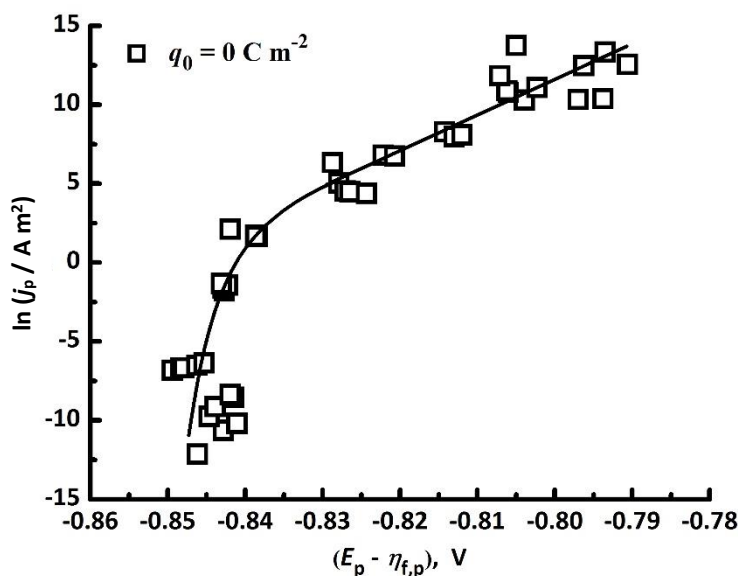The Tafel plot of the curve *j vs.* $E_{m/f}$ in Fig. 2 is represented in Fig. 3.

Fig. 3. *Tafel plot at the tin/oxide interface.*

In order to provide the best straight line region of the Tafel plot, the value of q_0 was taken equal to 2.5 C m^{-2}. Fig. 4 presents the obtained result.

From these results, the obtained Tafel slope (b_a) is equal to 41.995 mV dec^{-1}. By using Eq. (9) [21]

$$b_a = \frac{\alpha_{m/f} nF}{RT} \tag{9}$$

the transfer coefficients at the metal/film interface has been calculated as $\alpha_{m/f}$ = 1.07.
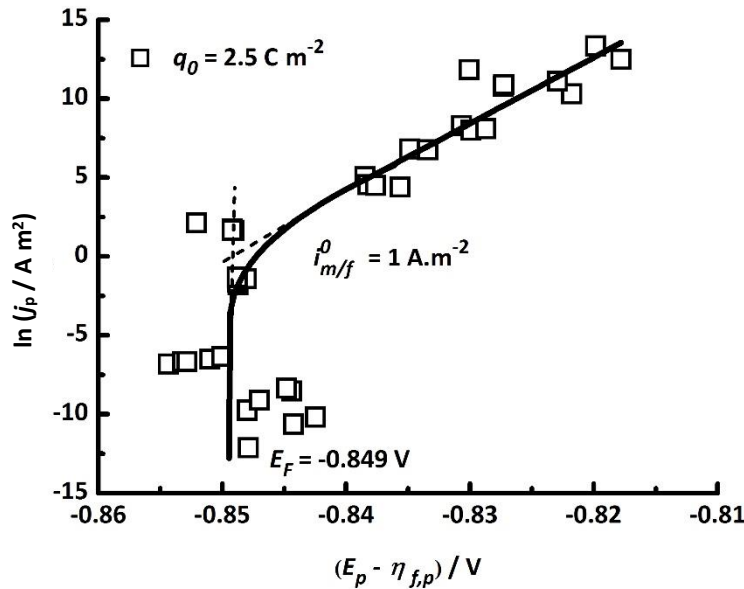
Fig. 4. *Tafel plot at the tin/oxide interface, considering* $q_0 = 2.5$ *C* m^{-2}.

Fig. 5 presents the corrected curve *j vs.* $E_{m/f,}$ which was obtained from the Tafel plot of Fig. 4. The anodic voltammograms are also shown in the same figure.
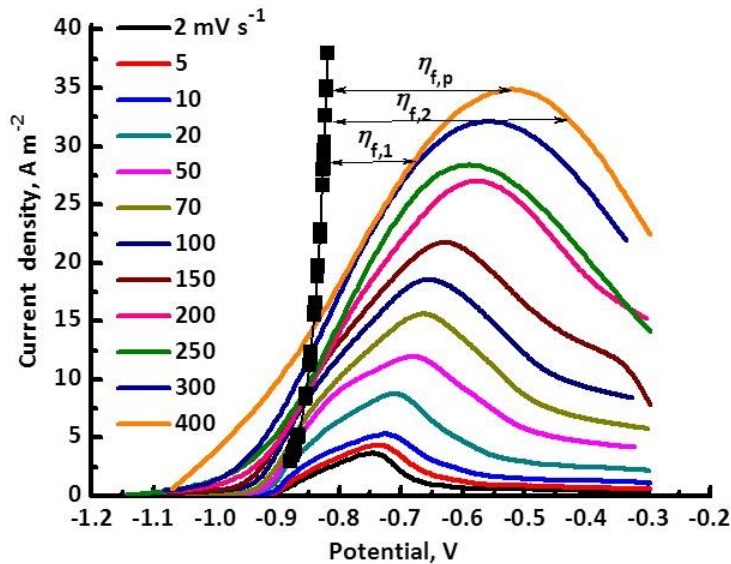

Fig. 5. *Voltammetric growths of tin oxide film, together with the plot of the calculated* j *vs.* (E − η$_f$) *relation at the metal/film interface, considering* q$_0$ = 2.5 *C* m^{-2} *and Figure 4.*

These results turn possible to determine the overpotential at the film (η_f) for any growing condition of the film beyond the peak condition. This can be done by calculating the difference of the potential in the voltammogram at any sweep rate and the potential in the curve *j vs.* $E_{m/f}$ for a given current density. This is shown in Fig. 5 for the voltammogram at 400 mV s^{-1}.

Thus, by calculating, η_f values for each potential of each voltammetry experiment, it becomes possible to determine the ionic specific resistivity of the film (ρ_f) and its variation with *E* and *v* using Eq. (6).

As was explained in the introduction of this work, the real values of V_f during the voltammetric growth could only be determined by an independent way of measuring the thickness of the film according to the following equation:

$$V_f = \frac{\ell A}{q_f}$$
(10)

In Eq. (10), ℓ is thickness and A is surface area the working electrode.

The thicknesses of oxides films grown at 2 mV s^{-1} were measured by ex-situ ellipsometry. This condition was chosen because using this sweep rate, higher thicknesses can be achieved. Fig. 6 presents the final potential (E_f) of each voltammetry experiment performed at 2 mV s^{-1}.
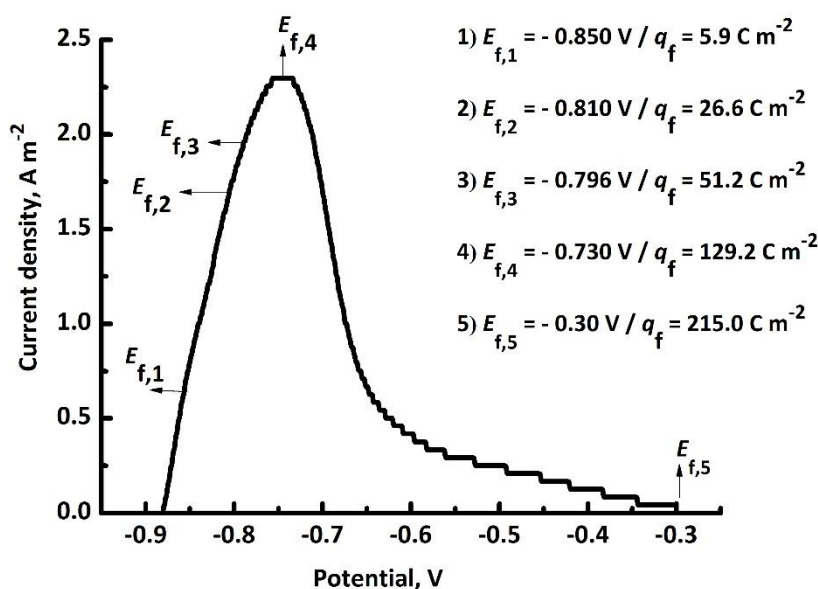

1) $E_{f,1}$ = - 0.850 V / q_f = 5.9 C m^{-2}

2) $E_{f,2}$ = - 0.810 V / q_f = 26.6 C m^{-2}

3) $E_{f,3}$ = - 0.796 V / q_f = 51.2 C m^{-2}

4) $E_{f,4}$ = - 0.730 V / q_f = 129.2 C m^{-2}

5) $E_{f,5}$ = - 0.30 V / q_f = 215.0 C m^{-2}

Fig. 6. *Voltammetric growth of tin oxide films at 2 mV s^{-1}, together with indication of the final potential, E_f, and corresponding film charge density values.*

As pointed out before, spectroscopic ellipsometer was used to obtain thin oxide film thicknesses for various charge densities. The proposed oxide layer structure is presented in Fig. 7. This oxide layer structure can be optically modelled using the both known refractive index (*n*) and extinction coefficient (*k*) of an available library (*nk* files) or dispersion relations for each of its layer constituents. Using the Drude and Gauss dispersion relations [16] for the film, the excellent fit was obtained between the used model and experimental data.
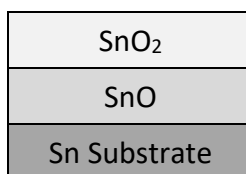

Fig. 7. *Model for the tin oxide layer structure.*

Fig. 8 exhibits typical results of fittings for measured and modelled values of tan Ψ and cos Δ for charge densities equal to 5.9 C m^{-2} and 215.0 C m^{-2}.
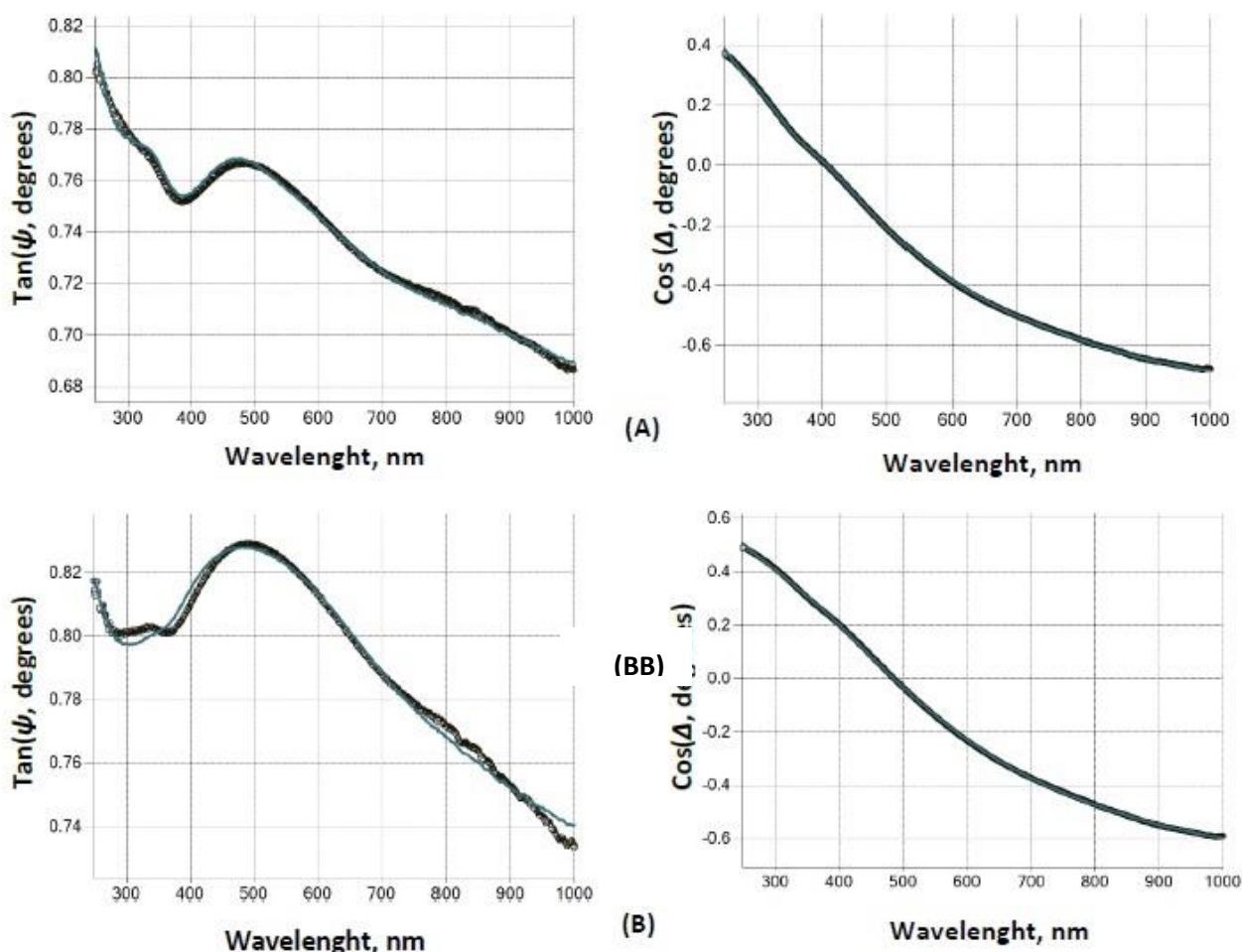
***Fig.8**. Typical plots of measured (open circles) and modelled (blue line) of tan (Ψ) and cos (Δ) for tin oxide films and charge densities equal to: (A) 5.9 C m^{-2} and (B) 215.0 C m^{-2}.*

It is clear from the graphs in Fig. 8 that excellent fits ($R^2 > 0.99$) were obtained, what make us confident to report the obtained thicknesses. The average thicknesses obtained considering eight measures at each charge density, are shown in Table 1. Except thicknesses, ℓ, in Table 1, one can also see values of the final potential, E_f, charge density of the film, q_f, and statistical results (R^2, as well as standard deviations of the average thickness values, σ). Data in Table 1 clearly show that for greater E_f and q_f, greater average film thickness is obtained.

***Table 1:** Final potentials, charge densities, thicknesses, average thicknesses and statistical results of calculations*

E_F / V	q_f / C m^{-2}	ℓ / nm								R^2	Average thicknesses, nm	σ
-0.850	5.9	3.8	3.8	3.5	3.5	3.0	3.1	3.0	3.3	**0.994**	**3.37**	**0.307**
- 0.810	26.6	4.3	3.8	4.6	4.5	3.9	4.0	3.8	3.7	**0.990**	**4.10**	**0.323**
- 0.796	51.2	4.3	4.5	4.6	4.1	3.9	4.3	4.1	4.5	**0.975**	**4.29**	**0.226**
- 0.730	129.2	9.4	9.0	9.3	8.9	9.4	9.0	9.3	9.1	**0.981**	**9.20**	**0.185**
- 0.300	215.0	10.7	11.6	10.3	11.3	10.3	11.0	12.2	10.8	**0.995**	**11.00**	**0.612**
0.100	268.1	13.7	12.5	13.2	12.9	12.4	11.2	11.8	11.5	**0.987**	**12.40**	**0.806**

In the preliminary experiment, a sample was left in the atmosphere during 24 h in order to measure the stabilized oxide film thickness and the resulting value was 2.0 nm. In Table 1, however, one can notice that the lowest average thickness for the film grown in conditions of voltammetric

experiments was 3.37 nm. This suggests that here obtained results are significantly influenced by the voltammetric way of film growth.

Using the experimentally found values of average thicknesses, Eq. (10) was applied and V_f was determined for the values of charge density of voltammetry grown films at 2 mV s^{-1}. The results are shown in Table 2 and Fig. 9.

Table 2: *Film volume per charge unit obtained from the thicknesses measurements of tin oxide films for different charge densities.*

q_f / C m^{-2}	ℓ / nm	V_f / 10^{-10} m^3 C^{-1}
5.9	3.37	5.70
26.6	4.10	1.54
51.2	4.29	0.84
129.2	9.20	0.71
215.0	11.00	0.50
268.1	12.40	0.46

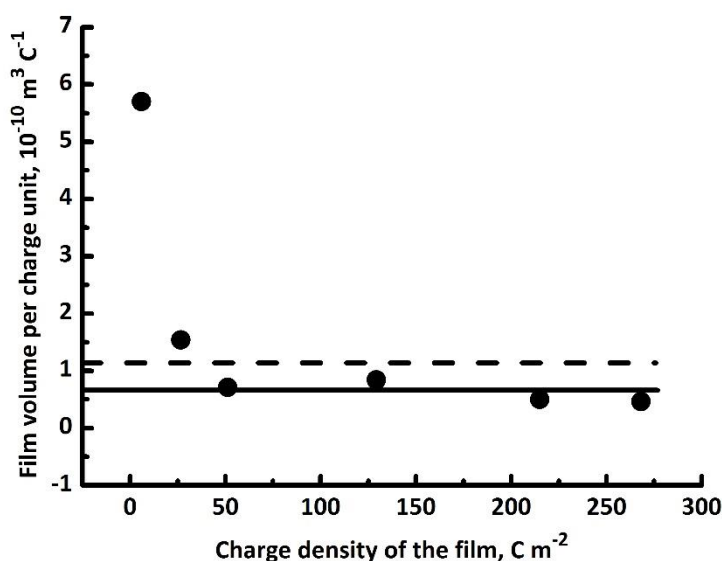**Fig. 9.** *Film volume per charge unit determined for different values of charge densities. (●) Experimental V_f, (---) V_f = 1.08×10^{-10} m^3 C^{-1} (considering SnO) and (–) V_f =0.568×10^{-10} m^3 C^{-1} (considering SnO$_2$)*

Data in Table 2 and Fig. 9 show that the values of V_f significantly decrease until 50 C m^{-2} of charge density of the film is achieved. This suggested that the film is less dense for lower values of charge density and becomes denser as the thickness increases [22]. Besides that, the value of V_f for charge density of 26.6 C m^{-2} is close to the value of V_f calculated by Eq. (7), considering a film of SnO (1.08×10^{-10} m^3 C^{-1}). For higher values of charge density, the value of V_f turns close to the value of V_f calculated considering a film of SnO$_2$ (0.568×10^{-10} m^3 C^{-1}). These results suggest that changes in the composition of the film are taking place as the potential turns more anodic. In fact, Duc and Tissot [23], studying the oxidation of tin in neutral phosphate solution, suggested that Sn(OH)$_2$ or SnO and Sn(OH)$_4$ or SnO$_2$ are present on the electrode surface at the beginning of polarization. At more anodic potentials only stannic species are formed. Electrochemical behavior of tin has also been studied in aqueous alkaline solutions [10–11,14,24–29]. The authors considered that primary passivation occurs due to formation of Sn(OH)$_2$ or SnO film by a dissolution-precipitation

mechanism. The final passivation is characterized by a continuous film of $Sn(OH)_4$ [10]. Then, more stables species like SnO_2 or $SnO_2.H_2O$ can be formed from dehydration of this last film [9]. Some authors have suggested a duplex film [28], consisting of $5SnO\ 2H_2O$ and $SnO_2.H_2O$ [29]. All these results emphasized importance of ellipsometric measurements in order to determine the thickness of the films. In fact, the exact composition of the film cannot be determined electrochemically.

By introducing experimentally determined V_f values into Eq. (6) the values of ρ_f can be calculated. Fig. 10 illustrates the results obtained using the values of charge density in Table 2 for the case of the voltammetry experiment at 2 mV s^{-1}.
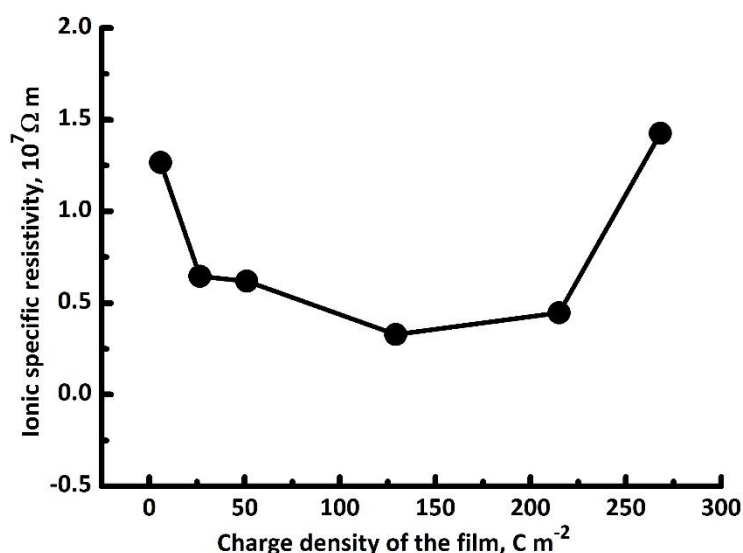

Fig. 10. *Ionic specific resistivity* vs. *charge density of the film for sweep rate equal to 2 mV s^{-1}.*

As can be observed in Fig. 10, ρ_f passes through a minimum (justifying the maximum in current densities). This behavior was also found by other authors for Zn, Nb, Ni and galvanized steel sheets [4–8]. According to the theory, this happens because the passage of current in the film of initial thickness (q_0) generates injection of specific defects, what resulted in decrease of ρ_f (inversely proportional to concentration of defects) [4–8]. Increase of recombining specific defects (interstitial and cationic vacancies) in the film ends up by generating the recombination reaction (interstitial cation + cationic vacancy → cationic net), and making ρ_f to increase again [4–8].

Conclusions

The ex-situ ellipsometric measurements of the thickness of tin oxides film grown by voltammetry experiments at 2 mV s^{-1} in the studied solution showed that the film is less dense for values of charge density below 50 C m^{-2} having V_f near 5.7×10^{-10} m^3 C^{-1}. For higher values of charge density, the film becomes denser having V_f near 0.5×10^{-10} m^3 C^{-1}.

From the experimentally determined values of V_f, the values of the variable ionic resistivity of the film during the voltammetric growth, ρ_f, were calculated. The behavior of ρ_f versus the charge density of the film was like that found by other authors in the cases of Zn, Nb, Ni and galvanized steel sheets.

Fluminense (UFF) for the opportunity of realizing this work, making the Laboratory of Electrochemical available.

Notation

A electrode surface area, m^2

b_a Tafel slope

E potential, V

E_F Flade potential, V

$E_{m/f}$ potential at the metal/film interface, V

F Faraday's constant, $C\ mol^{-1}$

j current density, $A\ m^{-2}$

j_p current density at the voltammetric peak, $A\ m^{-2}$

$j_{m/f}^{0}$ exchange current density at zero $\eta_{m/f}$, $A\ m^{-2}$

ℓ thickness of oxide layer, m

M molar mass of the film, kg

n number of electrons

q_f charge density of the film, $C\ m^{-2}$

q_0 charge density related to the amount of film initially present, at the beginning of the voltammetric growth on the metal surface, $C\ m^{-2}$

q_{volt} charge density related to the amount of film which has grown during voltammetric experiment, $C\ cm^{-2}$

$q_{f,p}$ peak or plateau charge density, $C\ cm^{-2}$

R gas constant, 8.314 J/mol K

SE spectroscopic ellipsometry

T temperature, K

V_f volume per charge unit, $m^3\ C^{-1}$

α_a anodic transfer coefficient

α_c cathodic transfer coefficient

δ density of the film, $kg\ m^{-3}$

$\eta_{m/f}$ overpotential at the metal/film interface

$\eta_{f.p}$ overpotential across the film at the voltammetric peak

η_f overpotential across the film

v sweep rate, $V\ s^{-1}$

ρ_f ionic specific resistivity of the film, $\Omega\ m$

References

[1]   A. S. Gliozzi, A. L. Alexe-Ionescu, G. Barbero, *Phys. Lett. A.* **379** (2015) 2657-2660.

[2]   A. L. Alexe-Ionescu , G. Barbero , S. Bianco, G. Cicero, C.F. Pirri, *J. Electroanal. Chem.* **669** (2012) 21-27.

[3]   G. Barbero, P. Batallioto, A. M. Figueiredo Neto, *J. Appl. Phys*. **101** (2007) 054102(1)-054102(5).

[4]   C. V. D'Alkaine, P. C. Tulio, M. A. C. Berton, *Electrochim. Acta* **49** (2004) 1989-1997.

[5]   C. V. D'Alkaine, L. M. N. Souza, F. C. Nart, *Corr. Sci.* **34** (1993) 129-149.

[6]   C. V. D'Alkaine, M. N. Boucherit, *J. Electrochem. Soc*. **10** (1997) 3331-3336.

[7]   C. V. D'Alkaine, M. A. Santanna, *J. Electroanal. Chem*. **457** (1998) 13-21.

[8]   T. B. Costa, C. V. D'Alkaine, T. M. C. Nogueira, 67th ABM International Congress, Voltammetric growth of ZnO on galvanized steel sheets containing Sb or Pb, Rio de Janeiro, Rio de Janeiro, 2012, p. 3162.

[9]   M. Pourbaix, Atlas of Electrochemical Equilibria in Aqueous Solution, Pergamon, Oxford, 1966.

[10] S. D. Kapusta, N. Hackerman, *Electrochim. Acta* **25** (1980) 1625-1639.

[11] M. Metikos-Hukovic, A. Resetic, V. Gvozdic, *Electrochim. Acta* **40** (1995) 1777-1779.

[12] T. Hurlen, *Electrochem. Acta* **39** (1994) 1359-1364.

[13] S. A. M. Refaey, *Electrochim. Acta* **41** (1996) 2545-2549.

[14] V. Brunetti, M. L. Teijelo, *J. Electroanal. Chem.* **613** (2008) 9-15.

[15] H. Fujiwara, *Spectroscopic Ellipsometry: Principles and Applications*. John Wiley & Sons Ltd, Tokyo, Japan, 2003.

[16] D. E. Aspnes, *Thin Solid Films* **571(3)** (2014) 334-344.

[17] K. Vedam, *Thin Solid Films* **313–314** (1998) 1 - 9.

[18] L. Arsov, I. Mickova, *J. Electrochem. Sci. Eng.* 5(4) (2015) 221-230.

[19] I. Arsova, Lj. Arsov, N. Hebestreit, A. Anders, W. Plieth, *J. Solid State Electrochem.* **11** (2007) 209-214.

[20] L. F. N. Guedes et al. J. Solid State Electrochem **20** (2016) 2517-2523.

[21] A. J. Bard and L. R. Faulkner, *Electrochemical Methods Fundamentals and Applications,* John Wiley & Sons, New York, United States, 2001.

[22] K. Wasa, M. Kitabatake, H. Adachi, *Thin films Materials Technology: sputtering of compound Materials*, William Andrew, New York, United States, 2004, p.28.

[23] H. Do Duc, P. Tissot, *Corros. Sci*. **19** (1979) 179-190.

[24] C. A. Gervasi, P. E. Alvarez, *Corros. Sci.* **47** (2005) 69 -78.

[25] S. D. Kapusta, N. Hackerman, *Electrochim. Acta* **25** (1980) 949-955.

[26] S. D. Kapusta, N. Hackerman, *Electrochim. Acta* **25** (1980) 1001-1006.

[27] S. D. Kapusta, N. Hackerman, *Electrochim. Acta* **25** (1982) 1886-1889.

[28] M. Metikos-Hukovic, M. Seruga, F. Ferina, Ber. Bunsenges, *Phys. Chem.* **96** (1992) 799-805.

[29] A. Ammar, S. Darwish, M. W. Khalil, S. El-Taher, *Electrochim. Acta* **33** (1988) 231-238.